

# Structural and Optical Properties of nanostructured Bismuth Sulfide-Lead Sulfide Thin Films of Variable Compositions

Omar H. Abd Elkader\*<sup>+</sup>

\*Physics Department, National Research Center, Cairo, Egypt

<sup>+</sup>Electron Microscope Unit, Zoology Department, College of Science, King Saud University, Riyadh 11451, Kingdom of Saudi Arabia

## ABSTRACT

Nanostructures thin films of six different compositions  $(\text{Bi}_2\text{S}_3)_{1-x}(\text{PbS})_x$  have been prepared by chemical bath deposition (CBD) from solution onto glass substrates. The nominal compositions in the range  $[0.1 \leq x \leq 0.85]$  were confirmed by Atomic Absorption Spectroscopy (AAS). X-Ray powder diffraction indicated different crystal structures for thin films of different compositions, while a large amorphous component was present. X-ray diffraction for as deposited and annealed samples showed that the crystallinity increases dramatically upon heat treatment of the thin films. The optical transmission spectrum of thin films deposited on glass substrates has been measured at room temperature [300 K], over the range from 300 nm to 2500 nm. The optical bandgaps  $[E_g]$  decrease with the addition of PbS. Annealing generally lowers the bandgaps of all films. Differential Scanning Calorimetry (DSC) showed that the major changes in the thin films started to proceed at temperatures between 570 and 750 K, depending on  $x$ .

## KEY WORDS

Nanostructures thin films, Chemical Bath Deposition, Optical properties, Thermal properties

## 1 - INTRODUCTION

Bismuth sulfide ( $\text{Bi}_2\text{S}_3$ ; optical band gap 1.9 eV), which has an orthorhombic structure [Pbnm space group] and lead sulfide (PbS optical band gap 0.3 eV), which has a rocksalt type structure [Fm3m space group], represent two different classes of chalcogenide semiconductors<sup>1, 2</sup>. They form bulk semiconductors in the pseudo-binary system  $(\text{Bi}_2\text{S}_3)_{1-x}(\text{PbS})_x$  up to  $x = 0.9$ , using a powder ingot method<sup>3, 6</sup>. These materials also occur as rare natural minerals in both amorphous and crystalline forms<sup>4</sup>. Structural properties of these minerals in bulk form have been investigated<sup>5</sup>. We have recently reported some interesting results of the morphology and electrical properties<sup>6</sup>. The study of thin films of semiconductors is important for applications in electronic and opto-electronic devices. Therefore, it is of interest to investigate the structural, thermal and optical properties of thin films in the system  $(\text{Bi}_2\text{S}_3)_{1-x}(\text{PbS})_x$ . In the present work, we report the chemical bath deposition of  $(\text{Bi}_2\text{S}_3)_{1-x}(\text{PbS})_x$  thin films from a single bath, with the objective of depositing films of different compositions, that can be utilized for heterojunction, photo- and electrochemical devices, IR detectors, and other applications. Co deposited metal sulfide thin films of Pb and Hg<sup>7</sup>, Cd and Pb<sup>8</sup> and Cu and Pb<sup>9</sup> have been reported by other research groups. The X-ray diffraction confirms the presence of  $(\text{Bi}_2\text{S}_3)$  (PbS) in the  $(\text{Bi}_2\text{S}_3)_{0.45}(\text{PbS})_{0.55}$  films, where the optical bandgaps indicate direct transition from valance band to conduction band and its value is 1.47 eV.

## 2 -EXPERIMENTAL DETAILS

### 2.1. PREPARATION OF THE THIN FILMS

The physiochemical bases of chemical deposition of metal chalcogenide thin films are discussed in<sup>10</sup>. In previous papers we reported the solution growth of  $(\text{Bi}_2\text{S}_3)$ <sup>11</sup> and (PbS)<sup>12</sup> thin films. In the present work, we have used 0.103 M  $\text{Bi}(\text{NO}_3)_3 \cdot 5\text{H}_2\text{O}$  and 0.175 M  $\text{Pb}(\text{NO}_3)_2$  dissolved in 3.7 M triethanolamine (TEA), which yielded a clear solution. Depositions were done in 100 ml beakers by using 20 ml of solution of  $\text{Bi}^{3+}$   $\text{Pb}^{2+}$ , 30 ml of 1 M Thiourea solution, 5 ml of 30%  $\text{NH}_3(\text{aq})$  and 45 ml distilled water. Four glass microscope slides were vertically supported in the beaker. The deposition could proceed at a temperature of 100 °C for duration of up to 5 hours. The resulting films were uniform over the entire substrate, with the thickness of the film increasing with the duration of deposition. We consider that the bath deposition method can be further optimized to reduce the duration of deposition.

### 2.2 CHARACTERIZATION OF THE FILMS

Chemical compositions were determined by atomic absorption spectroscopy (AAS), employing a Varian SPECTRA AA 220 instrument. Structural characterizations were done by x-ray powder diffraction (XRD). XRD was measured with a Philips X'pert diffractometer equipped with a primary monochromator to select  $\text{Cu-K}\alpha_1$  radiation. The diffraction was recorded in the range of 4 to 100° (2 $\theta$ ) using a step interval of 0.1°. The counting time was selected to yield a maximum intensity per step of 2000 to 3000 counts, resulting in 5 s per step. The Bragg-Brentano geometry allowed the thin films to be measured directly. Optical and thermal studies were carried out using UV- 2110 / 3101 PC system and Shimadzu DSC-50 system respectively.

### 3 - RESULTS AND DISCUSSION

#### 3.1 ATOMIC ABSORPTION SPECTROSCOPY

Spectroscopic methods of chemical analysis have become very widespread recently due to the sensitivity, and speed as compared with the conventional chemical method. Six powder samples  $(\text{Bi}_2\text{S}_3)_{1-x}(\text{PbS})_x$  [ $0.1 \leq x \leq 0.85$ ] were dissolved in concentrated nitric acid. Standard methods of analysis were used to determine the ratio  $x = \text{Pb} : \text{Bi}^{13}$ . Only small differences are found between nominal and experimental ratios (Table 1). Table 1. Composition  $x$  of  $(\text{Bi}_2\text{S}_3)_{1-x}(\text{PbS})_x$  [ $0.1 \leq x \leq 0.85$ ] as determined by atomic absorption spectroscopy (AAS).  $\Delta x$  indicates the difference between nominal and experimental values for  $x$ .

Table 1

| Nominal composition                                 | $x$ from AAS | $\Delta x$ |
|---|--------------|------------|
| $(\text{Bi}_2\text{S}_3)_{0.9}(\text{PbS})_{0.1}$   | 0.09         | 0009       |
| $(\text{Bi}_2\text{S}_3)_{0.75}(\text{PbS})_{0.25}$ | 0.248        | 0.002      |
| $(\text{Bi}_2\text{S}_3)_{0.6}(\text{PbS})_{0.4}$   | 0.348        | 0.052      |
| $(\text{Bi}_2\text{S}_3)_{0.45}(\text{PbS})_{0.55}$ | 0.553        | -0.003     |
| $(\text{Bi}_2\text{S}_3)_{0.3}(\text{PbS})_{0.7}$   | 0.755        | -0.055     |
| $(\text{Bi}_2\text{S}_3)_{0.15}(\text{PbS})_{0.85}$ | 0.835        | 0.015      |

#### 3.2 DIFFERENTIAL SCANNING CALORIMETRY (DSC)

The DSC curves for  $(\text{Bi}_2\text{S}_3)_{1-x}(\text{PbS})_x$  [ $0.1 \leq x \leq 0.85$ ] are shown in Figs. 1 through 3. Exothermic peaks are produced as a result of thermal transitions within the samples. The temperatures at which these peaks occur are summarized in Table 2.

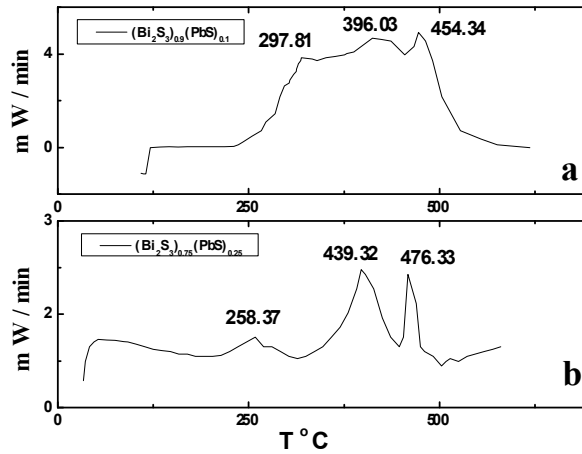


Fig. (1) DSC of chemically deposited  $(\text{Bi}_2\text{S}_3)_{1-x}(\text{PbS})_x$  powders (a)  $x = 0.1$ , and (b)  $x = 0.25$ .

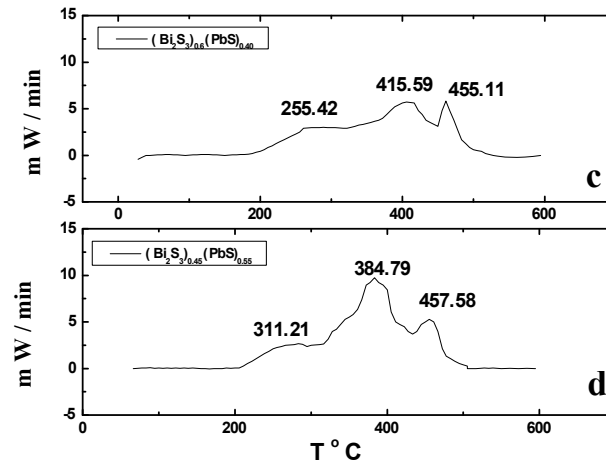


Fig (2) DSC of chemically deposited  $(\text{Bi}_2\text{S}_3)_{1-x}(\text{PbS})_x$  powders (c)  $x = 0.4$ , and (b)  $x = 0.55$ .

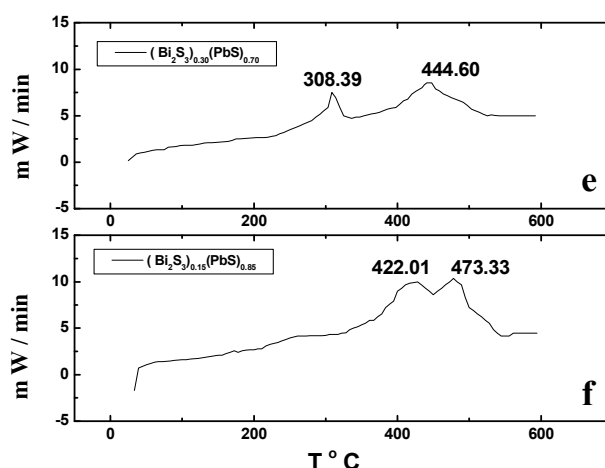


Fig (3) DSC of chemically deposited  $(\text{Bi}_2\text{S}_3)_{1-x}(\text{PbS})_x$  powders (e)  $x = 0.7$ , and (f)  $x = 0.85$ .

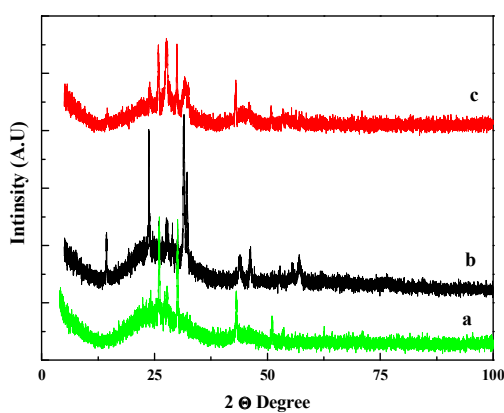
Table 2

| COMPOUND  | EXT. PEAK1 | EXT. PEAK 2 | EXT. PEAK3 |
|---|------------|-------------|------------|
| $(\text{Bi}_2\text{S}_3)_{0.9}(\text{PbS})_{0.1}$   | 297.81 °C  | 396.03 °C   | 454.34 °C  |
| $(\text{Bi}_2\text{S}_3)_{0.75}(\text{PbS})_{0.25}$ | 258.37 °C  | 439.32 °C   | 476.33 °C  |
| $(\text{Bi}_2\text{S}_3)_{0.6}(\text{PbS})_{0.4}$   | 255.42 °C  | 415.59 °C   | 455.11 °C  |
| $(\text{Bi}_2\text{S}_3)_{0.45}(\text{PbS})_{0.55}$ | 311.2 °C   | 384.79 °C   | 457.58 °C  |
| $(\text{Bi}_2\text{S}_3)_{0.3}(\text{PbS})_{0.7}$   | 308.39 °C  | -           | 444.60 °C  |
| $(\text{Bi}_2\text{S}_3)_{0.15}(\text{PbS})_{0.85}$ | 422.01 °C  | -           | 473.33 °C  |

The first exothermic peaks occur at temperatures that are consistent with the amorphous to crystalline transition. The temperature of this transitions varies with composition of  $(\text{Bi}_2\text{S}_3)_{1-x}(\text{PbS})_x$ , but for as deposited polycrystalline powder samples the first exothermic peaks interpreted as growth of grain size, the second and third exothermic peaks indicate that at higher annealing temperature a transformation to another crystalline state phase may occur.

### 3.3 X-RAY ANALYSIS:

Figure 4 a displays the X-ray diffraction patterns of the  $(\text{Bi}_2\text{S}_3)_{1-x}(\text{PbS})_x$  thin films of various compositions. The samples were heat treated under vacuum at a temperature 723 K for 4 hours. Lattice parameters together with the space group determined from the reflection conditions are given in Table 3 they indicate the major phase that is present in each sample.



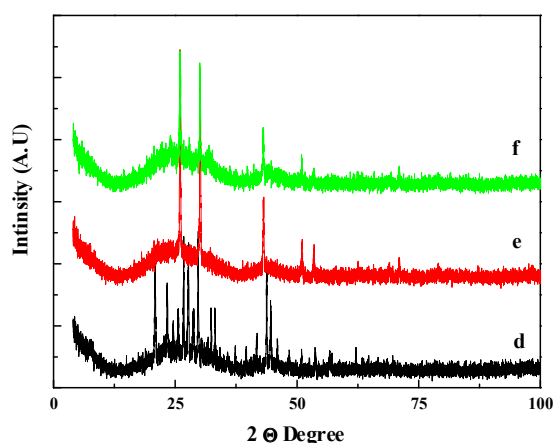


**Fig (4 a) XRD patterns of chemically deposited  $(\text{Bi}_2\text{S}_3)_{1-x}(\text{PbS})_x$  films at different ratios, annealed under vacuum at 723 K for 4 hour; a)x=0.1,b)x0.25,c)x0.4, d)x0.55,e)x0.7,andf)x = 0.85.**

Table 3 Lattice parameters as obtained from XRD. The phase is assigned in accordance with the lattice parameters of different mixed  $(\text{Bi}_2\text{S}_3)_{1-x}(\text{PbS})_x$  phases as they have been reported for bulk samples. Notice that  $\alpha = \beta = \gamma = 90$  degrees because of the orthorhombic and cubic symmetries.

Table 3

| <i>x</i><br><i>RATIO</i> | <i>a</i> | <i>b</i> | <i>c</i> | <i>VOLUME</i> | <i>SPACE GROUP</i> | <i>PHASE</i>            |
|--------------------------|----------|----------|----------|---------------|--------------------|-------------------------|
| 0.1                      | 11.0166  | 11.3568  | 3.95827  | 495.23        | Pbnm               | $\text{Bi}_2\text{S}_3$ |
| 0.1                      | 11.6534  | 14.9157  | 4.07903  | 709.01        | Pnam               | IV                      |
| 0.25                     | 11.2957  | 12.3224  | 3.935    | 547.71        | Pbam               | $\text{Bi}_2\text{S}_3$ |
| 0.4                      | 12.8857  | 13.3725  | 9.6222   | 1658.03       | P 222              | V                       |
| 0.55                     | 10.7854  | 13.954   | 8.4885   | 1277.52       | P 222              | IV                      |
| 0.7                      | 5.932    | 5.932    | 5.932    | 208.74        | Fm3m               | PbS                     |
| 0.85                     | 10.9876  | 11.3658  | 3.9591   | 494.43        | Pbnm               | $\text{Bi}_2\text{S}_3$ |
| 0.85                     | 5.932    | 5.932    | 5.932    | 208.74        | Fm3m               | PbS                     |

The difference between calculated lattice parameters for the thin films and those reported in the literature for bulk samples of the same nominal compositions  $(\text{Bi}_2\text{S}_3)_{1-x}(\text{PbS})_x$  can be due to the different methods of preparation. In this respect it is noticed, that in addition to the composite structure of alternating  $\text{Bi}_2\text{S}_3$  and PbS layers, a substantial fraction of Pb can be replaced by Bi without altering the PbS structure itself and these differences are influenced by the difference between the x ratio of (PbS) which indicated by atomic absorption spectroscopy.

### 3.4 SCANNING ELECTRON MICROSCOPY:

The grains or crystallites are formed by independent nucleation and growth processes randomly oriented and spaced with respect to one another. There is, in general, no epitaxial registration with the substrate lattice other than for nucleation occurring preferentially at defect sites and other surface irregularities. The grain size is controlled by the number of nucleating sites, which can increase by rapid quenching, by seeding with additives, or with highly abraded substrate surface. Grain growth. Annealing which reduces the grain boundary surface area by diffusion may then induce recrystallization. The surface morphology of a typical as deposited, and annealed at 623 K for 1 hour  $(\text{Bi}_2\text{S}_3)_{1-x}(\text{PbS})_x$  layers, which chemically deposited on glass substrate under different conditions are shown. The electron micrograph of the as deposited samples, demonstrate that films contain random distribution of well-defined small crystallites, it was noticed that as the temperature of annealing process increases, the dimensions of the crystallites are not uniform and an aggregate of islands with overgrowth scattered here, and there as shown in fig (4.b).

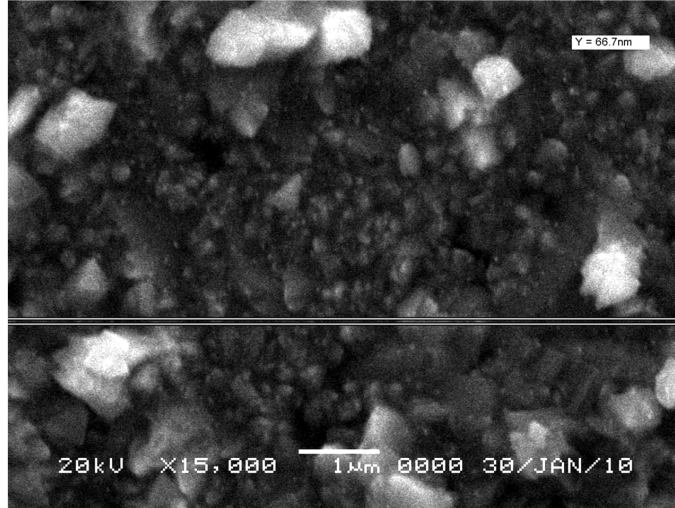


**Fig (4 b) Scanning Electron Microscopy of chemically deposited  $(\text{Bi}_2\text{S}_3)_{1-x}(\text{PbS})_x$  where  $x = 0.55$ .**

### 3.5 OPTICAL CHARACTERIZATION

Optical transmission spectroscopy of all samples was measured for wavelengths in the range 300-2500 nm. It is interesting to see the shift in absorption edge towards long wavelengths with increasing concentration PbS up to  $x = 0.55$  while for  $x = 0.7$  and  $0.85$  the shift goes towards short wavelengths. The thicknesses of the films were determined by microbalance method. The density of all films was calculated with the help of the formula:

$$\rho (\text{Bi}_2\text{S}_3)_{1-x} (\text{PbS})_x = \frac{1.6604 \times M (\text{Bi}_2\text{S}_3)_{1-x} (\text{PbS})_x \times Z}{V (\text{Bi}_2\text{S}_3)_{1-x} (\text{PbS})_x} \quad 1)$$

Where 1.6604 is the mass in grams of a hypothetical atom of atomic weight 1.000, M is the molecular weight of the sample, Z the number of molecules in each unit cell, and V is the volume of the unit cell in cubic angstrom.

The values of the absorption coefficient ( $\alpha$ ) and the extinction coefficients (k), as a function of the photon energy ( $h\nu$ ) were obtained from the measured transmission data and the calculated thicknesses. The absorption coefficient is of the order  $10^4 \text{ cm}^{-1}$  indicating that the films are of the direct-band gap type and the transitions are allowed. The variation of absorption coefficient as a function of the photon energy was found to obey the relation:

$$\alpha = B (h\nu - E_g)^{1/2} \quad 2)$$

Where B is a constant and  $E_g$  is the optical band gap. Figure 5 shows the calculated optical band gaps  $E_g$  of the thin films of  $(\text{Bi}_2\text{S}_3)_{1-x}(\text{PbS})_x$  annealed at 623 K for 1 hour. The optical band gap was determined by linear extrapolation to zero of the square of the absorption coefficient against the energy of the radiation. The optical band gap becomes smaller with an increasing concentration of PbS, in agreement with the smaller band gap of lead chalcogenide than of bismuth chalcogenide

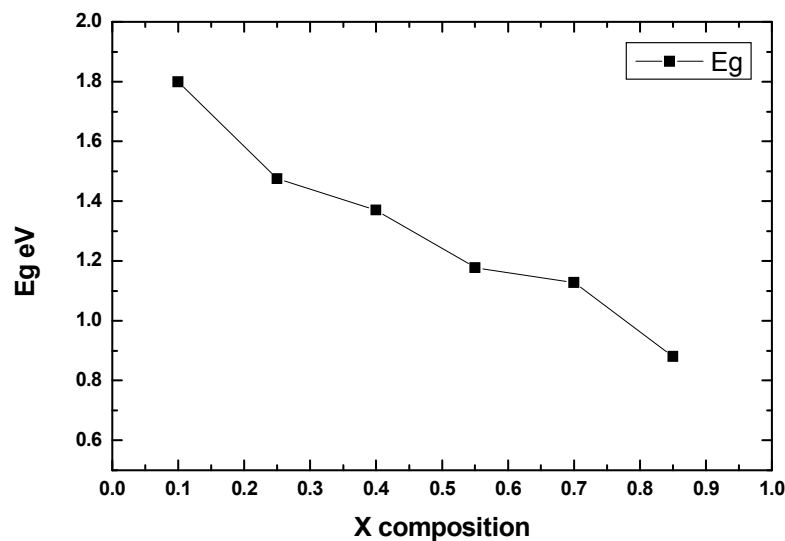


**Fig (5) Optical bandgaps of chemically deposited  $(\text{Bi}_2\text{S}_3)_{1-x}(\text{PbS})_x$  films at different ratios, annealed under vacuum at 623 K for 1 hour.**

#### REFERENCES

- [1] W.HOFMANN; Z.Kristallogr.,68,225(1933).
- [2] LANDOLT–BORNSTEIN Handbook [New Series 111/14b2] Berlin / Heidelberg: Springer-Verlag, 1986:301.
- [3] H.H OTTO and H. Strunz, N.Jb.Miner.Abh.108 (1), 1(1968).
- [4] JAMES R. Craig, Minera. Deposita 1, 278(1967).
- [5] J. TAKAGI and Y. Takeuchi, Acta cryst. B28, 649(1972).
- [6] S. MAHMOUD, M.A.Kenawy, S.Van Smallen, M.Wuttig and H. Omar, 7th Arab international conference on polymer science and technology and 3<sup>rd</sup> Arab conference on material science (ACMS-III) 2003.
- [7] N. C. SHARMA, D. K. Pandya, H. K. Sehgal, and K. L. Chopra, Mater. Res. Bull. 11,1109 (1976).
- [8] G. B. REDDY, D. K. Pandya, and K. L. Chopra, Solar Energy Mater. 15, 383 (1976).
- [9] R. SUAREZ and P.K. Nair, J. Solid. State. Chem. 123, (1996)296.
- [10] K. L. CHOPRA, R. C. Kanthla, D. K. Pandya, and A. P. Thakoor, Physics of thin films vol 12 (New Vourk: Academic) (1982)167.
- [11] S. MAHMOUD, A. H. Eid, and H. Omar, Fizika, A6 (3)(1996)111.
- [12]S. MAHMOUD, and H. Omar, Renewable Energy 24, (2001) 575.
- [13]APHA-AWWA-WPCF ‘Standard methods for the D.C., examination of water and wastewater’ Edition Washington American Public Health Association 17<sup>th</sup> edition (1989).